MULTISCALE MODEL. SIMUL.
Vol. 1, No. 3, pp. 349–370

IMAGE DECOMPOSITION AND RESTORATION USING TOTAL VARIATION MINIMIZATION AND THE H^{-1} NORM*

STANLEY OSHER†, ANDRÉS SOLÉ‡, AND LUMINITA VESE†

Dedicated to the memory of Andrés Solé, who died in a tragic accident soon after doing this work

Abstract. In this paper, we propose a new model for image restoration and image decomposition into cartoon and texture, based on the total variation minimization of Rudin, Osher, and Fatemi [*Phys. D*, 60 (1992), pp. 259–268], and on oscillatory functions, which follows results of Meyer [*Oscillating Patterns in Image Processing and Nonlinear Evolution Equations*, Univ. Lecture Ser. 22, AMS, Providence, RI, 2002]. This paper also continues the ideas introduced by the authors in a previous work on image decomposition models into cartoon and texture [L. Vese and S. Osher, *J. Sci. Comput.*, to appear]. Indeed, by an alternative formulation, an initial image f is decomposed here into a cartoon part u and a texture or noise part v. The u component is modeled by a function of bounded variation, while the v component is modeled by an oscillatory function, bounded in the norm dual to $|\cdot|_{H_0^1}$. After some transformation, the resulting PDE is of fourth order, envolving the Laplacian of the curvature of level lines. Finally, image decomposition, denoising, and deblurring numerical results are shown.

Key words. total variation, image decomposition, cartoon, texture, restoration, partial differential equation, functional minimization

AMS subject classifications. 35, 49

DOI. 10.1137/S1540345902416247

1. Introduction and motivations.

An important task in image processing is the restoration or reconstruction of a true image u from an observation f. Given an image function f defined on Ω, with $\Omega \subset \mathbb{R}^2$ an open and bounded domain, the problem is to extract u from f. The observation f is usually a noisy and/or blurred version of the true image. In order to solve this inverse problem in the denoising case, one of the most well-known techniques is by energy minimization and regularization. To this end, for $f \in L^2(\Omega)$, Rudin, Osher, and Fatemi [19] have proposed the following minimization problem:

$$\inf_u F(u) = \int_\Omega |\nabla u| + \lambda \int_\Omega |f-u|^2 dxdy. \tag{1.1}$$

Here, $\lambda > 0$ is a weight parameter, $\int_\Omega |f-u|^2 dxdy$ is a fidelity term, and $\int_\Omega |\nabla u|$ is a regularizing term to remove the noise. The term $\int_\Omega |\nabla u|$ is the total variation of u. If $u \in L^1(\Omega)$ and $\int_\Omega |\nabla u| < \infty$, then $u \in BV(\Omega)$, the space of functions of bounded variation (the gradient is taken in the sense of measures). This space allows for discontinuities along curves; therefore edges and contours are kept in the image u,

*Received by the editors October 16, 2002; accepted for publication (in revised form) May 5, 2003; published electronically July 17, 2003.
http://www.siam.org/journals/mms/1-3/41624.html

†Department of Mathematics, University of California Los Angeles, 405 Hilgard Avenue, Los Angeles, CA 90095-1555 (sjo@math.ucla.edu, lvese@math.ucla.edu). The research of the first author was supported in part by grants NSF DMS-0074735, ONR N00014-97-1-0027, and NIH P20MH65166. The research of the third author was supported in part by grants NSF ITR-0113439 and NIH P20MH65166.

‡The author is deceased. Former address: Departament de Tecnologia, Universitat Pompeu Fabra, Pg. de Circumval-lacio 8., Barcelona 08003, Spain. The research of this author was supported in part by PNPGC project, reference number BFM2000-0962-C02-01.

which is the minimizer of this convex optimization problem. Existence and uniqueness results of this minimization problem can be found in [1], [7], [20], [2].

Formally minimizing the functional (1.1) yields the associated Euler–Lagrange equation:

$$u = f + \frac{1}{2\lambda}\mathrm{div}\Big(\frac{\nabla u}{|\nabla u|}\Big) \text{ in } \Omega, \quad \frac{\partial u}{\partial \vec{n}} = 0 \text{ on } \partial\Omega.$$

This model performs very well for denoising of images, while preserving edges. However, smaller details, such as texture, are destroyed if the parameter λ is too small. To overcome this, Meyer [15] proposed a new minimization problem, changing in (1.1) the $L^2(\Omega)$-norm of $(f-u)$ by a weaker norm, more appropriate to represent textured or oscillatory patterns. This is defined as follows [15].

DEFINITION 1.1. *Let G denote the Banach space consisting of all generalized functions $f(x,y)$ which can be written as*

$$f(x,y) = \partial_x g_1(x,y) + \partial_y g_2(x,y), \quad g_1, g_2 \in L^\infty(\Omega), \tag{1.2}$$

induced by the norm $\|f\|_*$ defined as the lower bound of all $L^\infty(\Omega)$-norms of the functions $|g|$, where $\vec{g} = (g_1, g_2)$, $|g(x,y)| = \sqrt{g_1(x,y)^2 + g_2(x,y)^2}$, and where the infimum is computed over all decompositions (1.2) *of f.*

As Meyer mentions, the space G is the dual of the space $W^{1,1}(\Omega)$ (the set of functions f such that $\nabla f \in L^1(\Omega)^2$). He also introduces two other spaces, denoted by F and E. The space F is defined as G, but now g_1, g_2 belong to the John and Nirenberg space $BMO(\Omega)$, instead of $L^\infty(\Omega)$. Finally, the third space E considered by Meyer is defined as G, but g_1, g_2 belong to the Besov space $B_\infty^{-1,\infty}(\Omega)$. E coincides with $\dot{B}_\infty^{-1,\infty}(\Omega)$.

Meyer shows that if the component $v := f - u$ represents texture or noise, then it has to be modeled by one of these three larger spaces G, F, E. If $f - u \in G$, then he proposes the following new image restoration model:

$$\inf_u \Big\{ E(u) = \int_\Omega |\nabla u| + \lambda \|f - u\|_* \Big\}. \tag{1.3}$$

Note that this convex model cannot be solved directly, due to the form of the $*$-norm of $(f-u)$. We cannot express directly the associated Euler–Lagrange equation with respect to u.

In a recent work [21], the first and last authors have proposed a first practical method to overcome this difficulty. They have proposed the following convex minimization problem, as an approximation of (1.3):

$$\begin{aligned}\inf_{u,g_1,g_2} \Big\{ G_p(u,g_1,g_2) = \int_\Omega |\nabla u| + \lambda \int_\Omega |f - (u + \partial_x g_1 + \partial_y g_2)|^2 dxdy \\ + \mu \Big[\int_\Omega \Big(\sqrt{g_1^2 + g_2^2} \Big)^p dxdy \Big]^{\frac{1}{p}} \Big\},\end{aligned} \tag{1.4}$$

where $\lambda, \mu > 0$ are tuning parameters, and $p \to \infty$. As $\lambda \to \infty$ and $p \to \infty$, the first term ensures that $u \in BV(\Omega)$, and the second and third terms ensure that $\mathrm{div}\vec{g} \approx (f-u) \in G$. The minimization is made with respect to u, g_1, and g_2. Three coupled equations are then obtained from the computation of the associated Euler–Lagrange equations. In [21], image decomposition results into cartoon and texture,

and applications to texture discrimination have been proposed. For more details, we refer the reader to [21]. Note that if in (1.4) we take $p = 2$, with $v = \mathrm{div}\vec{g}$, $\vec{g} \in L^2(\Omega)$, then the quantity $\|v\| = \inf_{g_1,g_2 \in L^2(\Omega)} \sqrt{\int_\Omega (g_1^2 + g_2^2) dxdy}$ is exactly the seminorm of $H^{-1}(\Omega)$, the dual to $H_0^1(\Omega)$ (see, for instance, [10]). The minimization (1.4) yields the decomposition $f = u + v + w$, where $u \in BV(\Omega)$, $v = \mathrm{div}\vec{g}$ with small $\|\vec{g}\|_{L^p(\Omega)}$ norm, and the residual $w = -\frac{1}{2\lambda}\mathrm{div}(\frac{\nabla u}{|\nabla u|})$. In the limit, if $\lambda \to \infty$, then $\|w\|_{L^2(\Omega)} \to 0$. In [21], very satisfactory results of image decomposition into cartoon plus texture have been obtained even if λ is not too large.

In this paper, we propose an alternative practical approach, and we solve a simplified version of (1.3) and (1.4). We decompose f into $u + v$, with $u \in BV(\Omega)$, and $v = \triangle P$ a generalized function (a distribution) with small norm, dual to the seminorm of $H_0^1(\Omega)$. The precise formulation is given in the next section. Moreover, this new algorithm is a decomposition of the form $f = u + v$, while the original method [21] (which started this line of research) led to an $f = u + v + w$ model, with w a residual made as small as possible by increasing λ. In fact, $\|w\|_* \leq \frac{1}{2\lambda}$ (see [21]). The new algorithm is simplified; the minimization is performed only with respect to one unknown, u, and an interesting and new fourth order equation is obtained, equivalent to the proposed minimization model.

Recent related work is as follows: in Bertalmio et al. [4], an application of the model from [21] to image inpainting has been proposed. In Vese and Osher [22], the model from [21] is further analyzed and developed. Also, the authors Aujol et al. [3] have recently proposed an interesting model for image decomposition, following [15] and [21].

Related PDEs of fourth order, arising in image analysis, can be found, for instance, in [7], [12], and [11].

For more related details on the topic of oscillations in nonlinear analysis, we refer the reader to [17]. Other works for restoration of textured images by total variation minimization, in a wavelet framework, are by Malgouyres [13], [14]. Also, texture modeling by statistical methods was proposed by Zhu, Wu, and Mumford in [23], [24] and by Casadei, Mitter, and Perona in [5], among many others. In particular, we refer to Mumford and Gidas [16] for a stochastic model, in a related approach, for natural images. For more related references, we refer the reader to [21] and references therein.

For related results, alternative methods, and image decomposition methods using wavelets and harmonic analysis, we refer the reader to [15] and references therein.

The proposed new model is derived as follows.

2. Description of the proposed model. Assume that $f - u = \mathrm{div}\vec{g}$, with $\vec{g} \in L^2(\Omega)^2$. We can then formally assume the existence of a unique Hodge decomposition of $\vec{g}$ as

$$\vec{g} = \nabla P + \vec{Q},$$

where $P \in H^1(\Omega)$ is a single-valued function and $\vec{Q}$ is a divergence-free vector field. From here, we obtain that $f - u = \mathrm{div}\vec{g} = \triangle P$. Now, we express $P = \triangle^{-1}(f - u)$, and we propose the following new convex minimization problem, a simplified and modified version of (1.3):

$$\inf_u E(u) = \int_\Omega |\nabla u| + \lambda \int_\Omega |\nabla(\triangle^{-1})(f - u)|^2 dxdy. \tag{2.1}$$

This new minimization problem is obtained from (1.3) by neglecting $\vec{Q}$ from the expression for $\vec{g}$ and by considering the $(L^2\text{-norm})^2$ instead of the L^∞-norm for $|\vec{g}|$.

The precise formulations and assumptions are as follows. Consider the data

$$f \in BV(\Omega) + \left\{ v \in L^2(\Omega), \int_\Omega v(x,y)dxdy = 0 \right\}.$$

Then, by the embedding of $BV(\Omega)$ into $L^2(\Omega)$, we deduce that in fact $f \in L^2(\Omega)$.

We first recall the following theorem (see, for instance, [8]).

THEOREM 2.1. *Let $V_0 = \{P \in H^1(\Omega) : \int_\Omega P(x,y)dxdy = 0\}$. If $v \in L^2(\Omega)$, with $\int_\Omega v(x,y)dxdy = 0$, then the problem*

$$-\triangle P = v, \quad \frac{\partial P}{\partial n}|_{\partial\Omega} = 0, \tag{2.2}$$

admits a unique solution P in V_0.

Now, for each $v \in L^2(\Omega)$, with $\int_\Omega v(x,y)dxdy = 0$, there is a unique P with the properties from Theorem 2.1. We will express this as $P = \triangle^{-1}v$, and this gives a sense to the last term in (2.1).

This new minimization problem can therefore be written using the norm in $H^{-1}(\Omega)$, as defined by $\|v\|^2_{H^{-1}(\Omega)} = \int_\Omega |\nabla(\triangle^{-1})v|^2 dxdy$. Indeed, we can write

$$\inf_u E(u) = \int_\Omega |\nabla u| + \lambda \|f - u\|^2_{H^{-1}(\Omega)}. \tag{2.3}$$

Formally minimizing (2.1), we obtain the Euler–Lagrange equation:

$$2\lambda\triangle^{-1}(f-u) = \mathrm{div}\Big(\frac{\nabla u}{|\nabla u|}\Big), \quad \frac{\partial u}{\partial n}|_{\partial\Omega} = 0, \quad \frac{\partial \mathrm{div}\Big(\frac{\nabla u}{|\nabla u|}\Big)}{\partial n}|_{\partial\Omega} = 0. \tag{2.4}$$

Instead of directly solving (2.4), we apply the Laplacian to (2.4) to obtain

$$2\lambda(u-f) = -\triangle\Big[\mathrm{div}\Big(\frac{\nabla u}{|\nabla u|}\Big)\Big], \quad \frac{\partial u}{\partial n}|_{\partial\Omega} = 0, \quad \frac{\partial \mathrm{div}\Big(\frac{\nabla u}{|\nabla u|}\Big)}{\partial n}|_{\partial\Omega} = 0, \tag{2.5}$$

which we shall solve by driving to steady state

$$u_t = -\frac{1}{2\lambda}\triangle\Big[\mathrm{div}\Big(\frac{\nabla u}{|\nabla u|}\Big)\Big] - (u-f),$$

$$u(0,x,y) = f(x,y), \quad \frac{\partial u}{\partial n}|_{\partial\Omega} = 0, \quad \frac{\partial \mathrm{div}\Big(\frac{\nabla u}{|\nabla u|}\Big)}{\partial n}|_{\partial\Omega} = 0.$$

Remark. The assumption that $v := f - u$ satisfies $\int_\Omega (f-u)dxdy = 0$ is automatically satisfied by (2.5). This can be simply obtained by integrating the PDE in (2.5) in space and using integration by parts and the boundary condition on the curvature operator, in the sense of distributions. Therefore, by our model, the residual v satisfies the property of noise or texture of being of zero mean.

Remark. Let us justify now our procedure of minimizing (2.1) in a simple general framework to show that we still decrease the initial energy. Assume that we solve

$$\inf_u \int_\Omega F(u)dxdy.$$

Embedding the minimization in a dynamic scheme based on gradient descent, we obtain

$$u_t = -F_u.$$

We then replace this last equation by

$$u_t = \triangle F_u.$$

We show that the initial energy is still decreasing under the new flow. Indeed, we have

$$\begin{aligned}\frac{d}{dt}\left(\int_\Omega F(u)dxdy\right) &= \int_\Omega F_u u_t dxdy = \int_\Omega F_u \triangle F_u dxdy \\ &= \int_\Omega \operatorname{div}(F_u \nabla F_u)dxdy - \int_\Omega |\nabla F_u|^2 dxdy \\ &= \int_{\partial\Omega} F_u \frac{\partial}{\partial \vec{n}}(F_u)dS - \int_\Omega |\nabla F_u|^2 dxdy.\end{aligned}$$

This is a descent direction ($\frac{d}{dt}(\int_\Omega F(u)dxdy) < 0$) if

(a) $F_u = 0$ or $\frac{\partial}{\partial \vec{n}}(F_u) = 0$ on $\partial\Omega$,

(b) ∇F_u is not identically zero if F_u is not.

The condition (a) $\frac{\partial}{\partial \vec{n}}(F_u) = 0$ on $\partial\Omega$ is true in our framework. (b) is also true.

We believe that it is remarkable that a TV minimization model leads to an equivalent fourth order Euler–Lagrange PDE. Moreover, edges are kept in the u component, as we shall see in the numerical examples. Note that, by the Rudin–Osher–Fatemi (ROF) model, the curvature $k = \operatorname{div}(\frac{\nabla u}{|\nabla u|})$, defined in the generalized sense, satisfies $k \in L^2(\Omega)$, while by the new model, $k \in H^1(\Omega)$. So in the new model, the regularization is stronger than by the ROF model; therefore smaller details with the new model will be better separated from larger features. However, both models satisfy $\int_\Omega k(x,y)dxdy = 0$.

We also have the following interesting property of the residual $v := f - u$, where u is a minimizer of (2.1), giving information about vanishing moments. We state this simple result in the following theorem.

THEOREM 2.2. *Assume $f \in L^2(\Omega)$. For any subdomain Ω' of Ω, if u is the formal solution of* (2.4)*, then*

$$\int_{\Omega'} (f-u)w dxdy = 0$$

for each function $w \in H^1(\Omega')$ with $\triangle w = 0$ in Ω', as long as $K = 0$ and $\frac{\partial K}{\partial n} = 0$ on $\partial\Omega'$, where K denotes the curvature operator of level lines of u.

Proof. The proof of this theorem can be obtained by multiplying (2.5) by w and then integrating over Ω' in space and applying integration by parts. ∎

We can also show existence of minimizers for (2.1) as follows.

THEOREM 2.3. *For $f \in BV(\Omega) + \{v \in L^2(\Omega), \int_\Omega v(x,y)dxdy = 0\}$, the minimization problem*

$$\inf_u \left\{ F(u) = \int_\Omega |\nabla u| + \lambda \int_\Omega |\nabla \triangle^{-1}(f-u)|^2 dxdy, \quad \int_\Omega (f-u)dxdy = 0 \right\} \tag{2.6}$$

has a solution $u \in BV(\Omega)$.

Proof. Let u_n be a minimizing sequence of (2.6). Then there is a constant $M > 0$ such that $\int_\Omega |\nabla u_n| \leq M$ for all $n \geq 0$. By the Poincaré inequality, we obtain that there is a positive constant C, depending only on Ω, such that

$$\Big\| u_n - \frac{\int_\Omega u_n}{|\Omega|} \Big\|_{L^2(\Omega)} \leq C \int_\Omega |\nabla u|.$$

Since $\int_\Omega u_n = \int_\Omega f$, for all $n \geq 0$, we deduce that u_n is uniformly bounded in $L^2(\Omega)$, and therefore in $L^1(\Omega)$. Then we deduce that u_n is uniformly bounded in $BV(\Omega)$: there is a constant C' such that

$$\|u_n\|_{BV(\Omega)} = \|u_n\|_{L^1(\Omega)} + \int_\Omega |\nabla u| \leq C'.$$

Therefore, there is a subsequence of u_n, still denoted u_n, and $u \in BV(\Omega)$, such that $u_n \to u$ strongly in $L^1(\Omega)$ and weakly in $BV - w^*$, as $n \to \infty$. Moreover,

$$\int_\Omega |\nabla u| \leq \liminf_{n\to\infty} \int_\Omega |\nabla u_n|.$$

On the other hand, to each u_n of the minimizing and convergent subsequence (u_n) we can associate a unique $P_n \in H^1(\Omega)$, such that $f - u_n = -\triangle P_n$, from Theorem 2.1. We have that $\|\nabla P_n\|^2_{L^2(\Omega)} \leq M$, for all $n \geq 0$, and also that $\int_\Omega P_n dxdy = 0$. Again, by the Poincaré inequality, we obtain that

$$\Big\| P_n - \frac{\int_\Omega P_n}{|\Omega|} \Big\|_{L^2(\Omega)} = \|P_n\|_{L^2(\Omega)} \leq C \|\nabla P_n\|^2_{L^2(\Omega)} \leq C''$$

for all $n \geq 0$. Therefore, there is a subsequence of P_n, still denoted P_n, and $P \in H^1(\Omega)$, such that $P_n \to P$ in $L^2(\Omega)$, with $\int_\Omega P dxdy = 0$. In fact, by uniqueness of the limit, we need to have also $f - u = -\triangle P$. Therefore, we also have that

$$\|\nabla P\|^2_{L^2(\Omega)} = \|\nabla \triangle^{-1}(f-u)\|^2_{L^2(\Omega)} \leq \liminf_{n\to\infty} \|\nabla P_n\|^2_{L^2(\Omega)} = \|\nabla \triangle^{-1}(f-u_n)\|^2_{L^2(\Omega)}.$$

We finally deduce that

$$F(u) \leq \liminf_{n\to\infty} F(u_n);$$

therefore u is a minimizer of (2.6). Clearly, $\int_\Omega (f-u) dxdy = 0$. ∎

We will present numerical results of image denoising, obtained using the model (2.5), in section 4. Comparison with the standard models of Rudin, Osher, and Fatemi [19] and Vese and Osher [21] are also presented. We have also considered the restoration problem in the presence of both blur and noise. The original ROF model for restoring blurry, noisy imaging appeared in [18]. In this case, if $K : L^2(\Omega) \to L^2(\Omega)$ is a linear and continuous operator modeling the blur, and such that K^*, its adjoint operator, commutes with the Laplacian $\triangle$, then the model for deblurring and denoising is obtained in a similar manner: the convex energy to be minimized is

$$\inf_u E(u) = \int_\Omega |\nabla u| + \lambda \int_\Omega |\nabla(\triangle^{-1})(f - Ku)|^2 dxdy. \tag{2.7}$$

Following the same operations, we arrive at the transformed Euler–Lagrange equation

$$2\lambda(K^*Ku - K^*f) = -\triangle\Big[\mathrm{div}\Big(\frac{\nabla u}{|\nabla u|}\Big)\Big]. \tag{2.8}$$

We again solve this by our new descent procedure, which becomes

$$u_t = -\frac{1}{2\lambda}\triangle\Big[\mathrm{div}\Big(\frac{\nabla u}{|\nabla u|}\Big)\Big] - (K^*Ku - K^*f), \quad u(0,\cdot,\cdot) = f(\cdot,\cdot).$$

Note that if K is a convolution operator, then it commutes with the Laplace operator. Following [7] and [20], under appropriate assumptions on K, it is possible to modify the proof of Theorem 2.3 for the deblurring case (2.7).

Remark. We end this section by a simple but intuitive discussion and comparison of the norms in $H^{-1}(\Omega)$ used here and the G norm used by Meyer [15].

Consider $v : [0,1] \to \mathbb{R}$ such that $\int_0^1 v(x)dx = 0$. Then let $\hat{g}(x) = \int_0^x v(\xi)d\xi$. Let M, m be such that

$$M = \hat{g}(x_1) \geq \hat{g}(x) \geq \hat{g}(x_2) = m \text{ for all } x \in [0,1].$$

Then

$$\text{(A)} \qquad g(x) = \int_0^x v(\xi)d\xi - \Big(\frac{M+m}{2}\Big)$$

has the smallest $L^\infty[0,1]$-norm among all primitives of v, and

$$\|v\|_* = \frac{M-m}{2} = \frac{1}{2}\int_{x_2}^{x_1} v(\xi)d\xi.$$

For example, if $v = \sin 2\pi nx$, then $\|v\|_* = \|\sin 2\pi nx\|_* = \frac{1}{4\pi n}$.

Next, let P be such that $v = P''(x)$, with $P'(0) = P'(1) = 0$. Then $P'' = g'$, and

$$\text{(B)} \qquad g = P' = \int_0^x v(s)ds.$$

We have $\|v\|^2_{H^-1[0,1]} = \|g\|^2_{L^2[0,1]} = \int_0^1 (\int_0^x v(s)ds)^2$.

Note that the only difference between (A) and (B) is the constant $\frac{M+m}{2}$. Thus,

$$\|\sin 2\pi nx\|^2_{H^{-1}[0,1]} = \int_0^1 \Big(\frac{1-\cos 2\pi nx}{2\pi n}\Big)^2 dx = \frac{1}{4\pi^2 n^2}\frac{3}{2}.$$

In two dimensions, on the unit square, we can write

$$v = \sum_{n,m=1}^{\infty} a_{n,m}\cos 2\pi nx \cos 2\pi my.$$

Then

$$\triangle^{-1}v = -\sum_{n,m=1}^{\infty} a_{n,m}\frac{\cos 2\pi nx \cos 2\pi my}{n^2+m^2}$$

and

$$\|\nabla\triangle^{-1}v\|^2_{L^2(\Omega)} = \pi^2 \sum_{n,m=1}^{\infty} \frac{a^2_{m,n}}{n^2+m^2}.$$

3. Some additional theoretical results. We present in this section some theoretical results of the new model, similar to those mentioned by Meyer in [15], on the initial ROF model. We recall the notation $v := f - u$, with u a minimizer.

(I) $\|\triangle^{-1} f\|_* \leq \frac{1}{2\lambda}$ if and only if $u = 0$, $v = f$.

(II) $\|\triangle^{-1} f\|_* > \frac{1}{2\lambda}$ if and only if $\|\triangle^{-1} v\|_* = \frac{1}{2\lambda}$ and

$$-\int_\Omega (\triangle^{-1} v(x,y)) u(x,y) dxdy = \frac{1}{2\lambda} \|u\|_{BV(\Omega)},$$

where $\|u\|_{BV(\Omega)} = \int_\Omega |\nabla u|$ (recall that $v := f - u$).

Proofs.

(I) The minimizer is $u = 0$, $v = f$ if and only if, for any $h \in BV(\Omega)$,

$$\|h\|_{BV} + \lambda \|\nabla \triangle^{-1}(f - h)\|_2^2 \geq \lambda \|\nabla \triangle^{-1} f\|_2^2.$$

Expanding this inequality, we obtain

$$\|h\|_{BV(\Omega)} + \lambda \|\nabla \triangle^{-1} h\|_2^2 \geq -2\lambda \int h(\triangle^{-1} f) dxdy.$$

Replacing h first by $+\epsilon h$ and then by $-\epsilon h$, and letting $\epsilon \to 0$, we obtain

$$\|\triangle^{-1} f\|_* \leq \frac{1}{2\lambda}.$$

The inverse implication is also true: starting with this last inequality, then reversing the steps, we arrive at the desired inequality using (a) the fact that $\triangle^{-1} f \in L^2(\Omega)$ and (b) Lemma 3 from [21].

(II) We have

$$\|u + \epsilon h\|_{BV} + \lambda \|\nabla(\triangle^{-1}(v - \epsilon h))\|_2^2 \geq \|u\|_{BV} + \lambda \|\nabla \triangle^{-1} v\|_2^2;$$

then

$$\|u\|_{BV} + |\epsilon| \|h\|_{BV} + \lambda \|\nabla(\triangle^{-1}(v - \epsilon h))\|_2^2 \geq \|u\|_{BV} + \lambda \|\nabla \triangle^{-1} v\|_2^2.$$

Again, expand in the last inequality to get

$$|\epsilon| \|h\|_{BV} + \lambda \epsilon^2 \|\nabla \triangle^{-1} h\|_2^2 \geq -2\epsilon\lambda \int h \triangle^{-1} v dxdy.$$

Changing $\epsilon \to -\epsilon$ and taking $\epsilon \to 0$, we obtain, as before,

$$\|\triangle^{-1} v\|_* \leq \frac{1}{2\lambda}.$$

In the next step, we take $h = u$ in the first equation above. If $-1 < \epsilon < 1$, we have

$$\epsilon \|u\|_{BV} + \lambda \epsilon^2 \|\nabla \triangle^{-1} u\|_2^2 \geq -2\lambda\epsilon \int u \triangle^{-1} v dxdy.$$

If $\epsilon < 0$, we have

$$\|u\|_{BV} \leq 2\lambda \int u(-\triangle^{-1} v) dxdy.$$

If $\epsilon > 0$, then

$$\|u\|_{BV} \geq 2\lambda \int u(-\triangle^{-1}v)dxdy,$$

and therefore $\int u(-\triangle^{-1}v)dxdy = \frac{1}{2\lambda}\|u\|_{BV}$. This implies that $\|\triangle^{-1}v\|_* = \frac{1}{2\lambda}$.

Now, to verify the converse, we have

$$\begin{aligned}
&\|u + \epsilon h\|_{BV} + \lambda\|\nabla(\triangle^{-1}(v - \epsilon h))\|_2^2 \\
&\geq -2\lambda \int (\triangle^{-1}v)(u + \epsilon h) + \lambda\|\triangle^{-1}v\|_2^2 + 2\lambda\epsilon \int (\triangle^{-1}v)h + \lambda\epsilon^2\|\triangle^{-1}h\|_2^2 \\
&= -2\lambda \int (\triangle^{-1}v)udxdy + \lambda\|\triangle^{-1}v\|_2^2 + \lambda\epsilon^2\|\triangle^{-1}h\|_2^2 \\
&= \|u\|_{BV} + \lambda\|\triangle^{-1}v\|_2^2 + \lambda\epsilon^2\|\triangle^{-1}h\|_2^2 \\
&\geq \|u\|_{BV} + \lambda\|\triangle^{-1}v\|_2^2.
\end{aligned}$$

In the case of restoration and deblurring, if

$$\hat{u} = \underset{u}{\operatorname{argmin}} \|u\|_{BV} + \lambda\|\nabla\triangle^{-1}(Ku - f)\|_2^2,$$

then the analogous results are as follows:

(I) If $\|K^*\triangle^{-1}f\|_* \leq \frac{1}{2\lambda}$, then $\hat{u} = 0$ and $\hat{v} = f$.

(II) If $\|K^*\triangle^{-1}f\|_* \geq \frac{1}{2\lambda}$, then $\|K^*\triangle^{-1}\hat{v}\|_* = \frac{1}{2\lambda}$ and $(\hat{u}, K^*\triangle^{-1}\hat{v}) = -\frac{1}{2\lambda}\|\hat{u}\|_{BV}$.

The proofs for these results are similar.

Remark. Following Chambolle [6], we have an interesting characterization of the quantity $v = f - u$ for u the minimizer of our variational problem (2.1):

$$v = P^{(1)}_{K/2\lambda}(-\triangle^{-1}f) = \underset{w \in K/2\lambda}{\operatorname{argmin}} \int_\Omega (\nabla(w + 2\lambda\triangle^{-1}f))^2 dxdy.$$

Here

$$K = \{\mathrm{div}g |\ g \in L^2(\Omega)^2,\ \|g\|_\infty \leq 1\};$$

$P^{(1)}_{K/2\lambda}$ is the H^1 orthogonal projection onto $K/2\lambda$ of $-\triangle^{-1}f$. This result is obviously closely related with the results (I) and (II) above, just as Chambolle's original result [6] is related to Lemma 4 and Theorem 3, p. 32, of Meyer [15].

Again following Chambolle, we define

$$J(u) = \int |\nabla u| = \sup\left\{ \int_\Omega u\mathrm{div}\xi dxdy |\ \xi \in C_c^1(\Omega),\ \|\xi\|_\infty \leq 1 \right\}.$$

Then

$$J^*(u) = \sup_{u \in L^2(\Omega)} \int_\Omega (uv - J(u))dxdy = \begin{cases} 0 \text{ if } v \in K, \\ +\infty \text{ otherwise.} \end{cases}$$

Minimizing the functional defined in (2.1) gives us

$$-2\lambda\triangle^{-1}(f - u) \in \partial J(u),$$

where $\partial J(u)$ is the subdifferential of the functional $J(u)$ (see Ekeland and Temam [9] for the terminology). Since J is convex, by duality we obtain

$$u \in \partial J^*(-2\lambda \triangle^{-1}(f-u))$$

or

$$0 \in 2\lambda(f-u) - 2\lambda f + 2\lambda \partial J^*(-2\lambda \triangle^{-1}(f-u)).$$

Thus $w = -2\lambda \triangle^{-1}(f-u)$ is the minimizer of

$$\frac{\|\nabla(w + 2\lambda \triangle^{-1} f)\|^2}{2} + 2\lambda J^*(w).$$

This is our desired result.

4. Numerical results for image restoration. We present in this section our numerical results obtained with the proposed new model and comparisons with the TV model from [19]. In the experiments comparing our method with the classical TV model, the parameter λ has been chosen such that the L^2-norms of the v parts coincide. We also show comparisons with the original decomposition model introduced in [21].

In Figure 1, we show results obtained using both models on a textured image with a scale feature for different decreasing values of the parameter λ. The first row shows the minimizer u, while the third row shows $v := f - u$, respectively. The same experiment has been performed using the classical TV model; the second row shows the minimizer u_{TV}, while the fourth row shows $v_{TV} := f - u_{TV}$. The parameter λ for the case of the TV model has been selected in each case in order to accomplish $\|v_{TV}\|_2 = \|v\|_2$. We note that the new model separates better the textured details from the larger regions: the small textured details are in the v component, while the larger regions are kept in the u component. Using the standard TV model, small textured details are still kept in the u_{TV} component, while contours of larger regions can be seen in the v_{TV} component; therefore, the separation between texture and nontexture is not that well made using the standard TV model. These remarks can be seen on the third column in Figure 1.

The same experiment has been performed on an image composed of four different Brodatz textures (see Figure 2). The corresponding u, v, u_{TV}, and v_{TV} are displayed in Figure 3 (recall that in the TV result λ has been chosen such that $\|v_{TV}\|_2 = \|v\|_2$). The same remarks can be made by looking at these results: the new model separates better the nontexture details, represented in u, from the texture details, represented in v (compare the right upper squares of the u components in Figure 3, top and bottom). We also show in Figure 4 the absolute value of v and v_{TV} (after histogram equalization for visualization purposes).

Figure 5 corresponds to a real image where there is a high presence of textures combined with nontextured parts. We have made the same kind of experiment as for the Brodatz textures, which are shown in Figures 6 and 7, respectively. The u and v components are displayed in Figure 6, while the absolute value of the v components is displayed in Figure 7. Again, we can make the same observation: the new model separates better the textured details shown in v from nontextured images kept in u. Indeed, if we look to the v components from Figure 6, we still see the hands in the result produced by the standard TV model. These are not seen in the v component produced by the new model. On the other hand, details like the eyes are much better

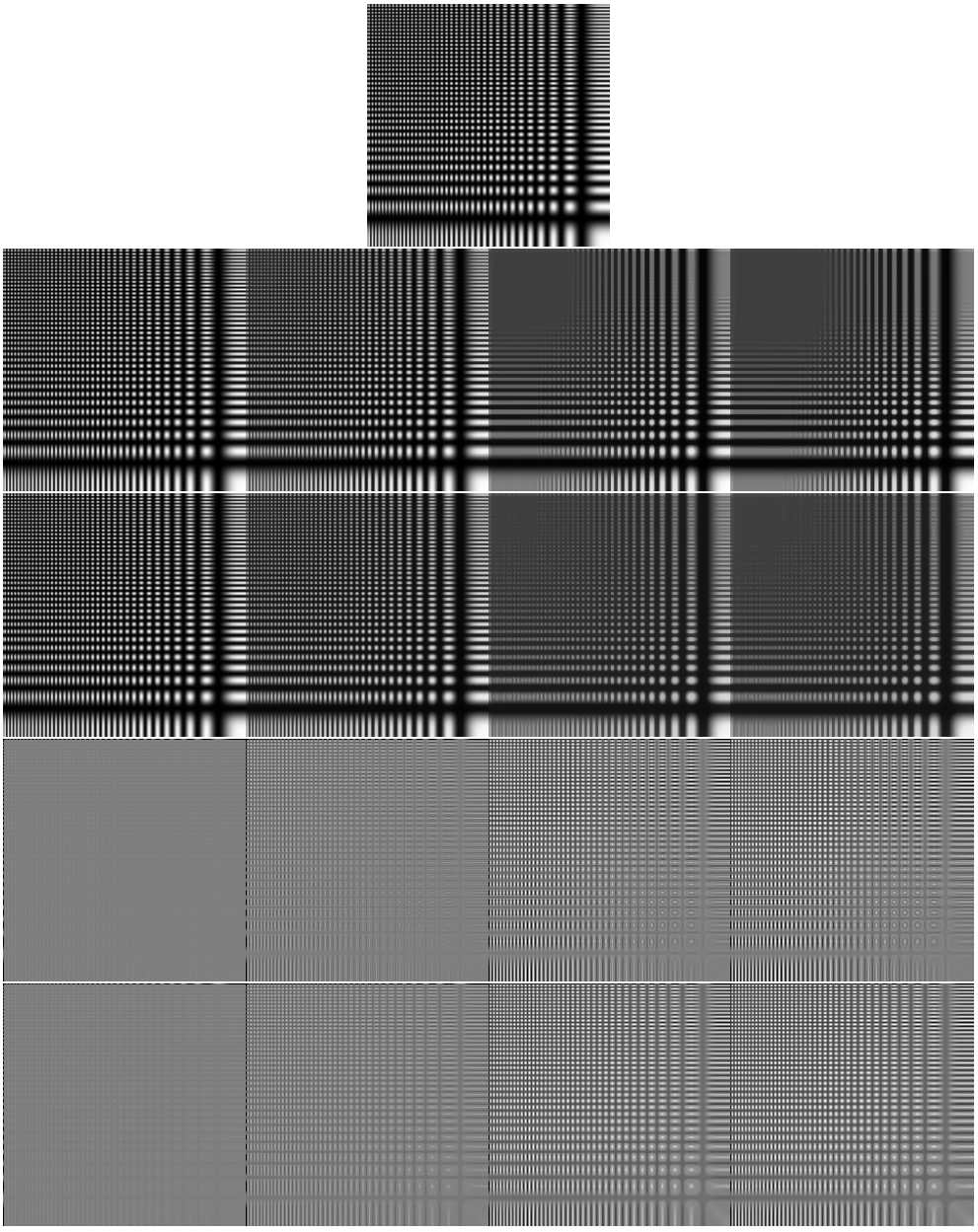

FIG. 1. *Top: original grid image. First row: from left to right, computed u for $\lambda = 1, 0.1, 0.001, 0.0001$ with the new model. Second row: computed u for the TV model. Third row: computed v for the new model. Fourth row: computed v for the TV model. In each case the TV result has been computed such that the L^2-norm of v is the same as in the new model.*

kept in the u component of the new model. These remarks can also be noticed in Figure 7. In other words, the new model performs much better in keeping the main contours in the u component, instead of the v component. The new model performs better for separating the main larger features from the textured features. We also show in Figure 6 a comparison with the model from [21] (obtained very fast, using

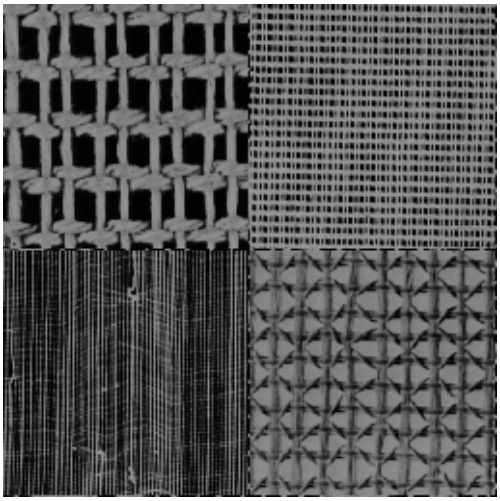

FIG. 2. *Original image composed of four different Brodatz textures.*

only 100 time iterations). From these comparisons, we note that, on this image, the present new model has fewer edges in the v component, thus giving again a very good result. More comparisons with the original model [21] are presented in Figure 8, where the two image decomposition models give slightly different but comparable results.

Figures 9, 10, and 11 show the performance of the new model compared with the classical TV model for the denoising problem. Figure 9 corresponds to the woman image before and after corrupting it with white Gaussian noise of standard deviation 10. Figure 10 shows the denoised image using our approach and the classical TV model. In both cases the parameter λ has been computed using the gradient projection method in order to satisfy the constraint $\|f_{noise} - u\|^2 = \sigma^2$ (although there is no proof on the convergence of λ using the gradient projection method; in practice it seems to work). Figure 11 just shows a zoom of a textured part of the image.

We present also some results concerning the deblurring/denoising problem using the woman image (Figures 12 and 13) and the satellite image (Figures 14 and 15). If we carefully compare the results from Figure 15, together with the PSNR and the RMSE, we see that the new model performs better in this denoising-deblurring case.

Finally, we end this section with a decomposition result on an image with an object with fractal boundary (corresponding to the "Sierpinsky pentagon"), using the new model. The result of the decomposition is remarkable, as shown in Figure 16: the cartoon part is well represented in the component u, while the oscillatory fractal-like boundaries are kept in the v component. We plan to extend this example to decomposition and representation of shapes in three dimensions in a future work. The shape will be represented by characteristic functions f.

5. Conclusion. In this paper, we have proposed a new model for image restoration and image decomposition into cartoon plus texture, which combines the total variation minimization from the ROF model [19] with a norm for oscillatory functions proposed by Meyer [15] involving the H^{-1} norm. The new model performs better on textured images, and the "residual" component v has less structure than in the standard TV model. We also present some theoretical analysis of the model.

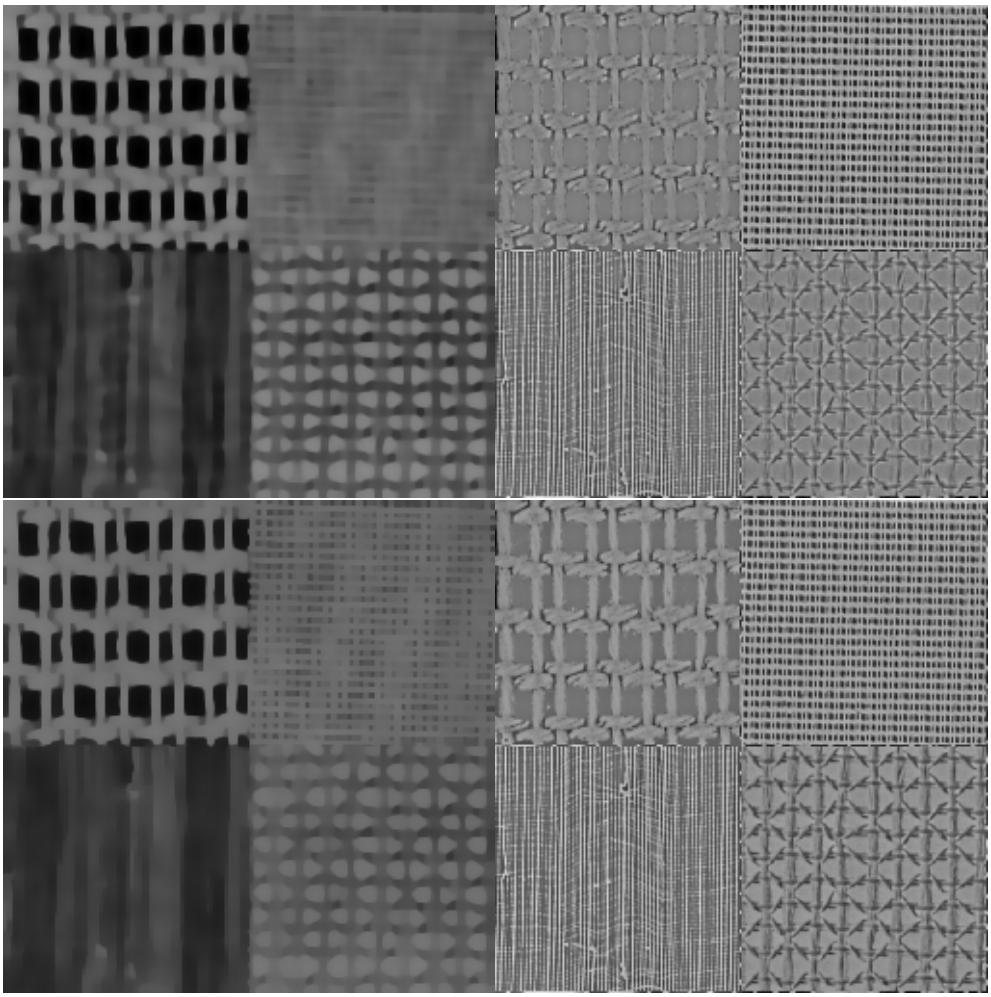

FIG. 3. *Top: Decomposition into u (left) and v (right) using our method. Bottom: Decomposition into u (left) and v (right) using the TV model. In order to compare we have chosen λ in the TV model such that the L^2-norm of v is the same in both cases.*

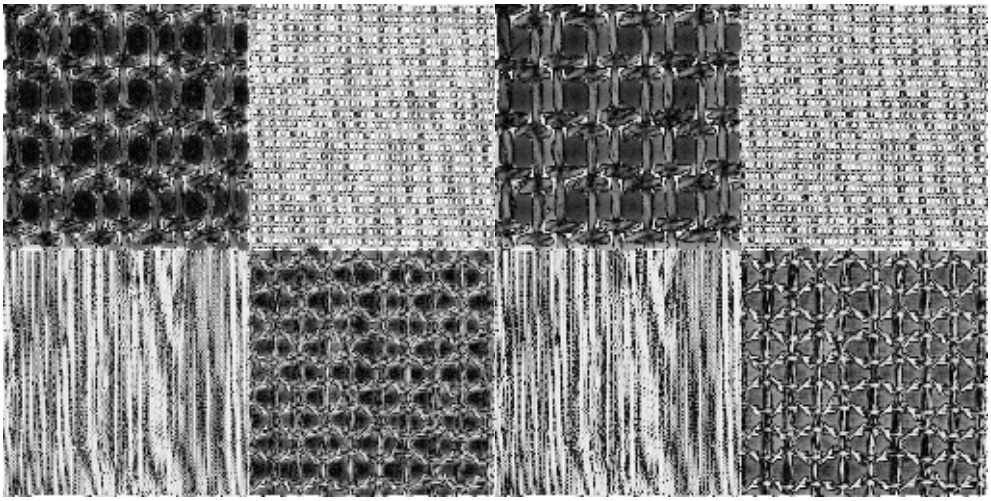

FIG. 4. *Absolute value of v in our case (left) and for the TV model (right). An equalization of the histogram has been performed for visualization purposes.*

FIG. 5. *Original woman image.*

FIG. 6. *u (left) and v (right) using the new method (top), the TV model (middle), and* [21] *(bottom). We choose* λ *in the TV model such that the* L^2*-norm of v is the same in the first and second rows.*

FIG. 7. *Absolute value of v in our case (left) and for the TV model (right). An equalization of the histogram has been performed for visualization purposes.*

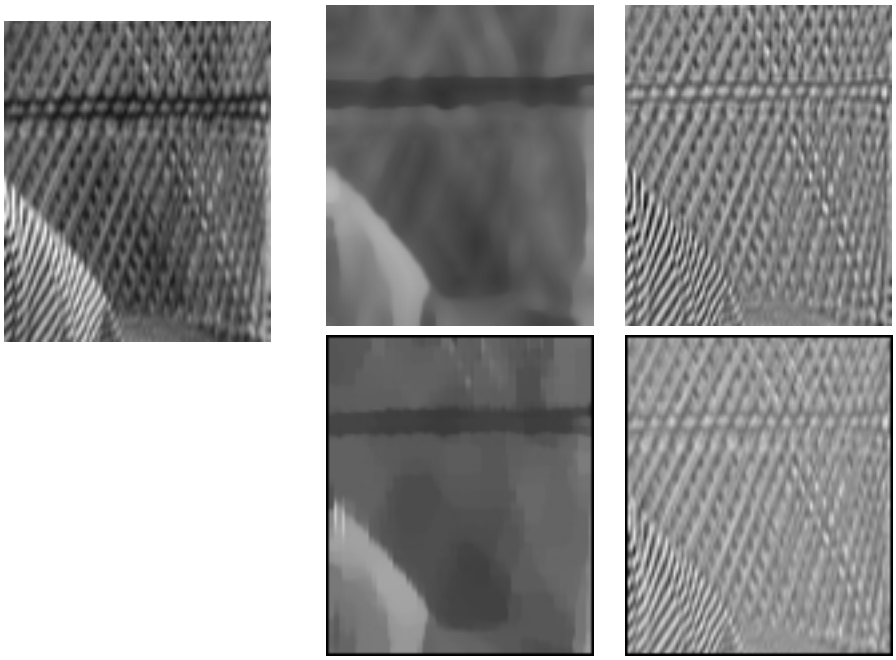

FIG. 8. *More comparisons with the model* [21] *from* (1.4). *Top: the proposed new model.*

FIG. 9. *Original woman image (left) and corrupted image with white Gaussian noise of* $\sigma = 10$ *(right).*

FIG. 10. *Left: denoised image using the new model. Right: denoised image using the TV model.*

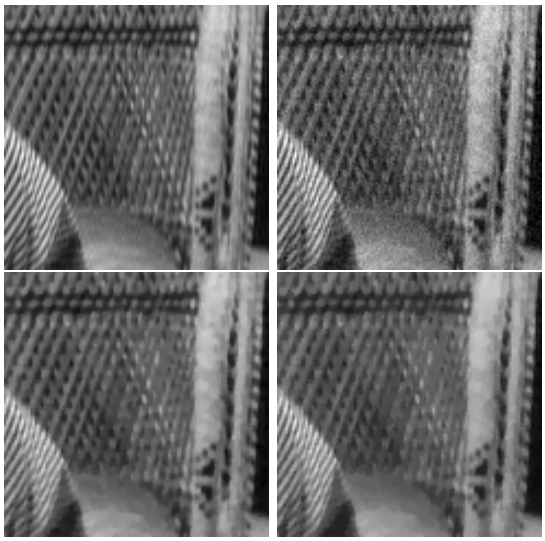

FIG. 11. *Zoom of a textured zone, from left to right, top to bottom: original, noisy, denoised with the new model, denoised with the TV model.*

FIG. 12. *Original image (left) and the corrupted image (Gaussian blur of* $\sigma = 3$ *plus additive Gaussian noise of* $\sigma = 1$*).*

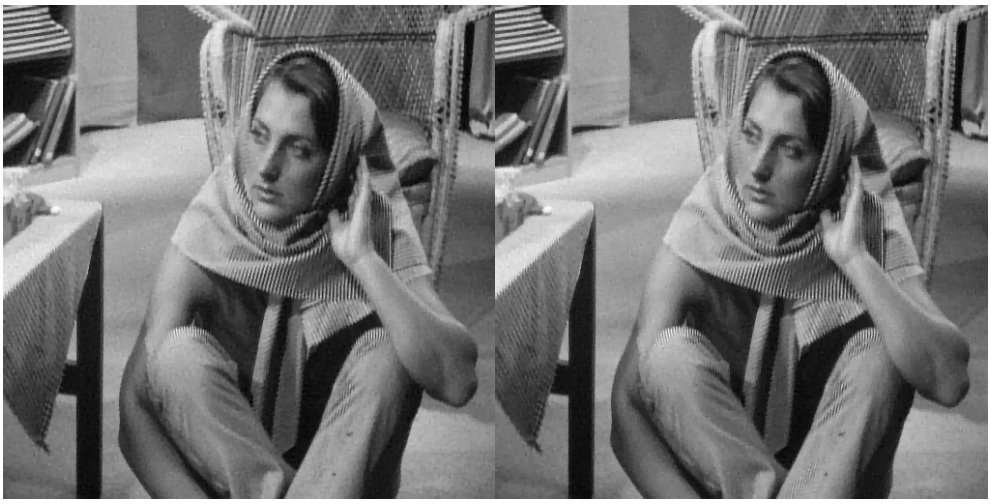

FIG. 13. *Restoration using the proposed model (left) and the TV model (right).*

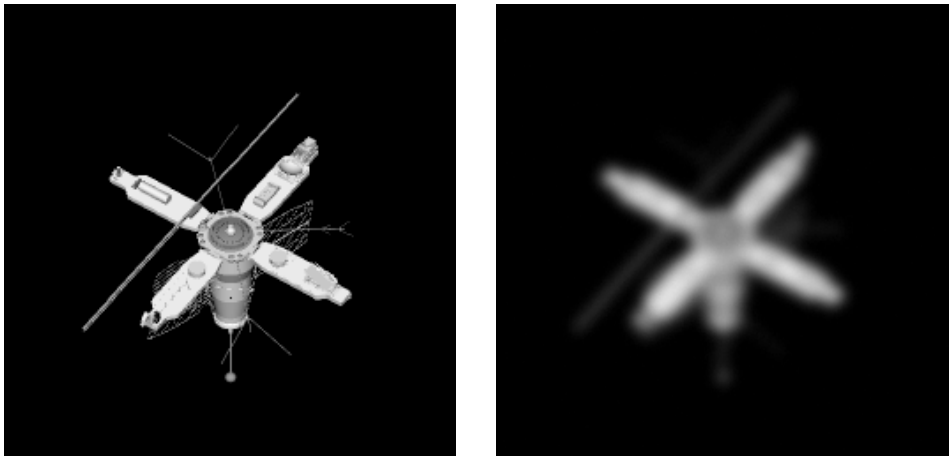

FIG. 14. *Original image (left) and the corrupted image (Gaussian blur of* $\sigma = 4$ *plus additive Gaussian noise of* $\sigma = 1$*). The values for the PSNR (peak to signal to noise ratio) and the RMSE (root mean square error) are, respectively,* $PSNR = 21.66dB$ *and* $RMSE = 0.0826$.

FIG. 15. *Restoration using the proposed model (left, PSNR* $= 24.10dB$ *and RMSE* $= 0.0624$*) and the TV model (right, PSNR* $= 23.98dB$ *and RMSE* $= 0.0633$*). Observe that the proposed model gives a slightly better result (higher PSNR and lower RMSE) than the classical TV model.*

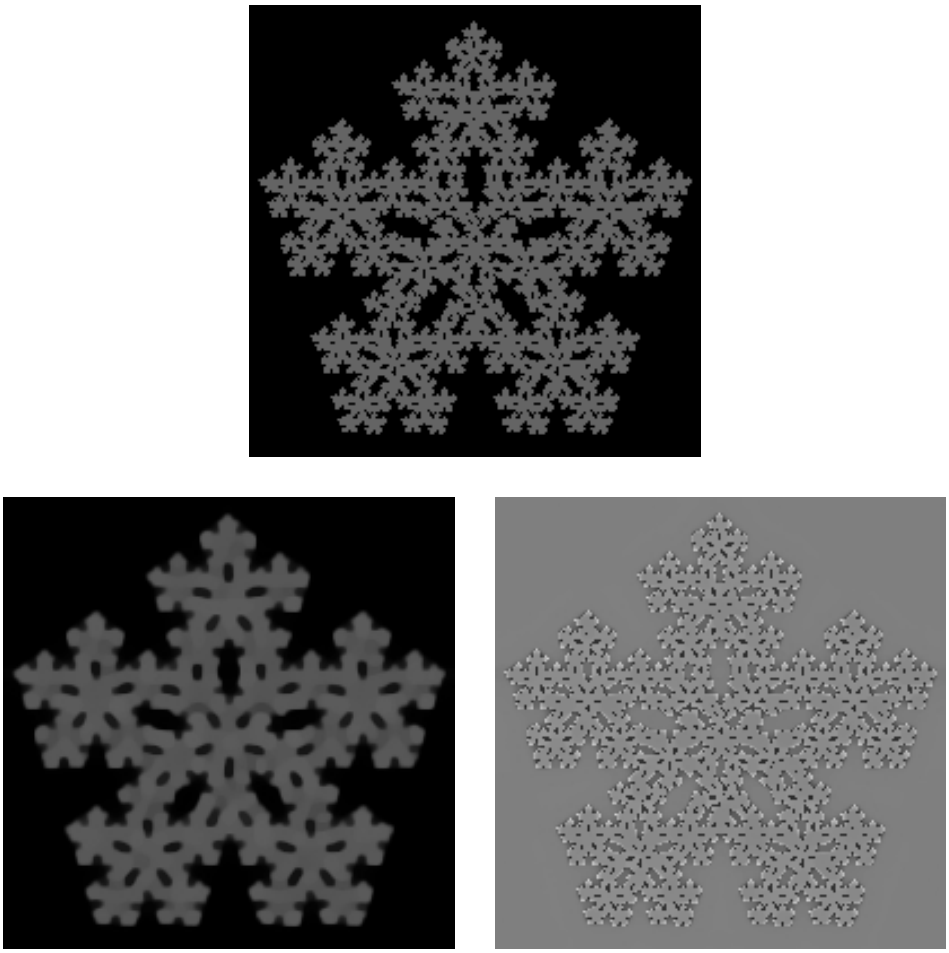

FIG. 16. *Decomposition of an image with an object with fractal boundary (corresponding to the "Sierpinsky pentagon") using the new model. Top: f; bottom left: u; bottom right: v.*

Acknowledgments. The authors would like to thank A. Marquina, from the University of Valencia, Spain, for providing us the satellite image, and V. Caselles, A. Chambolle, and Y. Meyer for their helpful comments on the first draft of the paper.

REFERENCES

[1] R. Acart and C.R. Vogel, *Analysis of bounded variation penalty methods of ill-posed problems*, Inverse Problems, 10 (1994), pp. 1217–1229.
[2] F. Andreu, C. Ballester, V. Caselles, and J.M. Mazon, *Minimizing total variation flow*, C. R. Acad. Sci. Paris Sér. I Math., 331 (2000), pp. 867–872.
[3] J.-F. Aujol, G. Aubert, L. Blanc-Féraud, and A. Chambolle, *Image Decomposition: Application to Textured Images and SAR Images*, Rapport de Recherche RR 4704, INRIA, Sophia-Antipolis Cedex, France, 2003.
[4] M. Bertalmio, L. Vese, G. Sapiro, and S. Osher, *Simultaneous structure and texture image inpainting*, IEEE Trans. Image Process., to appear.
[5] S. Casadei, S. Mitter, and P. Perona, *Boundary detection in piecewise homogeneous textured images*, in Computer Vision—ECCV '92, Lecture Notes in Comput. Sci. 588, Springer-Verlag, Berlin, 1992, pp. 174–183.
[6] A. Chambolle, *An algorithm for total variation minimization and applications*, J. Math. Imaging Vision, to appear.
[7] A. Chambolle and P.L. Lions, *Image recovery via total variation minimization and related problems*, Numer. Math., 76 (1997), pp. 167–188.
[8] R. Dautray and J.-L. Lions, *Mathematical Analysis and Numerical Methods for Science and Technology, Vol.* 2*, Functional and Variational Methods*, Springer-Verlag, Berlin, 1988.
[9] Y. Ekeland and R. Temam, *Analyse Convexe et Problèmes Variationnels*, Dunod, Gauthier-Villars, Paris, 1974.
[10] L.C. Evans, *Partial Differential Equations*, Grad. Stud. Math. 19, AMS, Providence, RI, 1998.
[11] J.B. Greer and A.L. Bertozzi, H^1 *Solutions of a Class of Fourth Order Nonlinear Equations for Image Processing*, UCLA CAM Report 03-11, UCLA, Los Angeles, CA, 2003.
[12] M. Lysaker, A. Lundervold, and X.-C. Tai, *Noise Removal Using Fourth-Order Partial Differential Equations with Applications to Medical Magnetic Resonance Images in Space and Time*, UCLA CAM Report 02-44, UCLA, Los Angeles, CA, 2002.
[13] F. Malgouyres, *Mathematical analysis of a model which combines total variation and wavelet for image restoration*, J. Information Processes, 2 (2002), pp. 1–10.
[14] F. Malgouyres, *Minimizing the total variation under a general convex constraint for image restoration*, IEEE Trans. Image Process., 11 (2002), pp. 1450–1456.
[15] Y. Meyer, *Oscillating Patterns in Image Processing and Nonlinear Evolution Equations*, Univ. Lecture Ser. 22, AMS, Providence, RI, 2002.
[16] D. Mumford and B. Gidas, *Stochastic models for generic images*, Quart. Appl. Math., 59 (2001), pp. 85–111.
[17] F. Oru, *Le rôle des oscillations dans quelques problèmes d'analyse non-linéaire*, Thèse, CMLA, ENS-Cachan, Cachan cedex, France, 1998.
[18] L. Rudin and S. Osher, *Total variation based image restoration with free local constraints*, in Proceedings of the IEEE ICIP 1994, Vol. I, Austin, TX, pp. 31–35.
[19] L. Rudin, S. Osher, and E. Fatemi, *Nonlinear total variation based noise removal algorithms*, Phys. D, 60 (1992), pp. 259–268.
[20] L. Vese, *A study in the BV space of a denoising-deblurring variational problem*, Appl. Math. Optim., 44 (2001), pp. 131–161.
[21] L. Vese and S. Osher, *Modeling textures with total variation minimization and oscillating patterns in image processing*, J. Sci. Comput., to appear.
[22] L. Vese and S. Osher, *Image denoising and decomposition with total variation minimization and oscillatory functions*, J. Math. Imaging Vision, to appear.
[23] S.C. Zhu, Y.N. Wu, and D. Mumford, *Filters, random fields and maximum entropy (FRAME): Towards a unified theory for texture modeling*, Internat. J. Computer Vision, 27 (1998), pp. 107–126.
[24] S.C. Zhu, Y.N. Wu, and D. Mumford, *Minimax entropy principle and its application to texture modeling*, Neural Computation, 9 (1997), pp. 1627–1660.